



Geophysical Research Letters®



RESEARCH LETTER

10.1029/2021GL095602

Key Points:

- Seasonal forecasting models do not have skill in simulating North American Monsoon (NAM) rainfall
- We use a data driven weather type (WT) algorithm to identify synoptic situations associated with NAM rainfall on catchment scales
- The frequency of monsoonal flow WTs days allows for the skillful forecast of NAM season rainfall starting in April

Supporting Information:

Supporting Information may be found in the online version of this article.

Correspondence to:

A. F. Prein, prein@ucar.edu

Citation:

Prein, A. F., Towler, E., Ge, M., Llewellyn, D., Baker, S., Tighi, S., & Barrett, L. (2022). Sub-seasonal predictability of North American Monsoon precipitation. *Geophysical Research Letters*, 49, e2021GL095602. https://doi.org/10.1029/2021GL095602

Received 5 AUG 2021 Accepted 22 MAR 2022

© 2022. The Authors.

This is an open access article under the terms of the Creative Commons Attribution License, which permits use, distribution and reproduction in any medium, provided the original work is properly cited.

Sub-Seasonal Predictability of North American Monsoon Precipitation

Andreas F. Prein¹ , Erin Towler¹, Ming Ge¹, Dagmar Llewellyn², Sarah Baker³, Shana Tighi³, and Lucas Barrett²

¹National Center for Atmospheric Research (NCAR), Boulder, CO, USA, ²Bureau of Reclamation (Upper Colorado Region), Albuquerque, NM, USA, ³Bureau of Reclamation (Lower Colorado Region), Boulder, NV, USA

Abstract North American Monsoon (NAM) rainfall is a vital water resource in the United States Southwest, providing 60–80% of the region's annual precipitation. However, NAM rainfall is highly variable and water managers lack skillful guidance on summer rainfall that could help inform their management decisions and operations. Here we show that NAM season (June–October) precipitation can be forecasted by the European Centre for Medium-Range Weather Forecast's model months ahead at catchment scales. This is possible by identifying the frequency of days with synoptic-scale moisture advection into the NAM region, which greatly improves predictability over directly utilizing modeled precipitation. Other forecasting systems fail to provide useful guidance due to deficiencies in their data assimilation systems and biases in representing key synoptic features of the NAM including its teleconnections.

Plain Language Summary Managing freshwater resources in the United States (U.S.) Southwest is difficult due to the region's large year-to-year precipitation variability and increasing population density. Additionally, climate change is expected to reduce the region's water availability making the efficient management of water a necessity. However, the lack of skill in predicting regional precipitation on sub-seasonal to seasonal timescales makes it extremely difficult to reach this goal. We use state-of-the-art seasonal forecasts to investigate their skill in predicting North American Monsoon season rainfall. Consistent with previous studies, we find that the models fail in forecasting rainfall in the region. However, using the frequency of atmospheric moisture surges into the U.S. Southwest as a proxy for rainfall results in skillful predictions starting in April. This novel forecasting method will allow regional water managers to make more informed decisions and can mitigate the impacts of droughts and floods in the future.

1. Introduction

The U.S. Southwest is a global hotspot for water scarcity (Liu et al., 2017; Mekonnen & Hoekstra, 2016) and is currently battling one of its most severe droughts in decades. With diminishing water resources from snowmelt (Ikeda et al., 2021; Milly & Dunne, 2020; Mote et al., 2005; Rasmussen et al., 2011) and steadily increasing population and freshwater demand (MacDonald, 2010), U.S. Southwest water resource managers are interested in potential opportunities from the secondary source of rainfall from the North American Monsoon (NAM). The NAM contributes approximately 35%–45% to the annual precipitation in the desert Southwest (Higgins et al., 1999) and up to 60% in New Mexico. However, NAM rainfall is extremely variable on inter-seasonal (Carleton, 1986), inter-annual (Carleton et al., 1990; Higgins et al., 1998, 1999; Higgins & Shi, 2000), and decadal time-scales (Castro et al., 2001; Yu & Wallace, 2000).

Meteorologically, the NAM is related to the poleward propagation of the subtropical high, that is, the monsoon high, over North America, which starts in May and June in Mexico and is centered over New Mexico in July and August (Adams & Comrie, 1997; Higgins et al., 1998). This shift results in anomalous flow patterns from the southeast over Arizona and New Mexico, transporting warm and moist air from the Gulf of Mexico and the Pacific Ocean onto the continent. This leads to convective precipitation and a distinct summer maximum in the precipitation annual cycle. The onset of the monsoon in Arizona and New Mexico is variable but typically happens in early July. The NAM season is characterized by intermittent monsoonal moisture surges and dry spells related to shifts in the monsoonal high pressure system (Higgins et al., 2004; Jiang & Lau, 2008; Pascale & Bordoni, 2016; Schiffer & Nesbitt, 2012; Seastrand et al., 2015).

PREIN ET AL.

Predicting NAM precipitation on seasonal to sub-seasonal (S2S) time scales remains challenging. Historic observations show that NAM characteristics are modulated by Pacific sea surface temperature patterns (Castro et al., 2001). Observations also show that wet winters tend to be followed by dry monsoon seasons and vice versa in New Mexico and Arizona (Gutzler & Preston, 1997; Higgins et al., 1998). However, tree-ring reconstructions covering the last five centuries indicate that this link is weak, at best, and not stable over time (Griffin et al., 2013). Zhu et al. (2005) found no significant relationships between the antecedent soil moisture conditions during NAM onset and total precipitation. Additionally, S2S forecasting systems have no significant skill in predicting precipitation in the U.S. Southwest after two to 3 weeks of leadtime (Krishnamurti et al., 2002; Li & Robertson, 2015; Slater et al., 2019). The dominant processes that could contribute to S2S predictability of early season NAM precipitation are warm-season atmospheric teleconnection modes such as the West Pacific North America pattern or quasi-stationary Rossby wave trains (Castro et al., 2012; Ciancarelli et al., 2014). These teleconnections influence the positioning and seasonality of the monsoon high and thereby the amount of precipitation in the region (Carleton et al., 1990).

In many snowmelt-driven basins in the Western U.S., operational seasonal water supply forecasts decisions are mainly based upon snowpack and don't explicitly consider any information about monsoon precipitation due to its low predictability. Skillful forecasting products that intersect with decision points on seasonal and annual planning horizons are extremely valuable to water managers and are a research priority (Bureau of Reclamation, 2018, 2021; Raff et al., 2013).

Here we present a forecasting framework that leverages the ability of current seasonal forecasting systems in simulating large-scale circulation patterns that are associated with monsoonal rainfall rather than utilizing erroneously modeled rainfall directly (Crochemore et al., 2016). The goal of this study is to establish a set of weather types (WTs) that can be used in a seasonal forecasting framework to investigate the potential to predict NAM precipitation variability. Therefore, we use a novel data-driven weather typing algorithm based on clustering (Prein & Mearns, 2021) that uses objective criteria to identify archetypal WTs. Specifically, we derive WTs that are optimized for NAM precipitation in catchments in Arizona and New Mexico, which include the Lower Colorado River Basin and Rio Grande Basin, respectively. The algorithm tests many combinations of atmospheric predictor variables, establishing the optimal set of WTs from two skill scores based on the precipitation average and standard deviation of the derived WTs. Similar approaches have been shown to provide novel insights into the origin of precipitation changes on climate time scales (Lehner et al., 2017; Prein et al., 2016). Further, we investigate the potential for skillful forecasts of NAM season rainfall by examining the ability of seasonal forecasts to predict the identified WTs, versus predicting precipitation directly.

2. Data and Methods

2.1. Season and Region of Interest

We investigate June to October conditions, which incorporates the core monsoon season from July to September and helps to assess the onset and decay of the monsoonal high. Our focus region includes eight catchments in Arizona and six in New Mexico (Figure 1a). Those catchments were selected due to their importance for water management in these states. We derive WTs for each of these catchments based on the skill scores discussed below.

2.2. Observations and Reanalysis

We use the Parameter-elevation Regressions on Independent Slopes Model (PRISM, Daly et al., 1997) gridded daily precipitation data for calculating precipitation statistics. PRISM provides data for the 1982–2018 period on a 4 km horizontal grid over the conterminous United States.

For the WT classification, we use daily average atmospheric variables from ECMWF's Interim Reanalysis within the period 1982–2018 (Dee et al., 2011). The selection of predictor variables is limited by variables that are commonly stored by seasonal forecasting centers; we include the following 12 variables in the analysis: sea level pressure, 850 hPa zonal, meridional, and total wind speed, 850 hPa and 500 hPa moisture flux, water vapor mixing ratio, and air temperature, 500 hPa geopotential height, and 200 hPa wind speed. The same variables are also important on weather forecast timescales, as they related to dynamic forcing and thermodynamic instability.

PREIN ET AL. 2 of 11

19448007, 2022. 9, Downloaded from https://agupubs.onlinelibrary.wiley.com/doi/10.1029/2021GL095602, Wiley Online Library on [28/04/2023]. See the Terms and Conditions (https://onlinelibrary.wiley.com/terms

for rules of use; OA articles

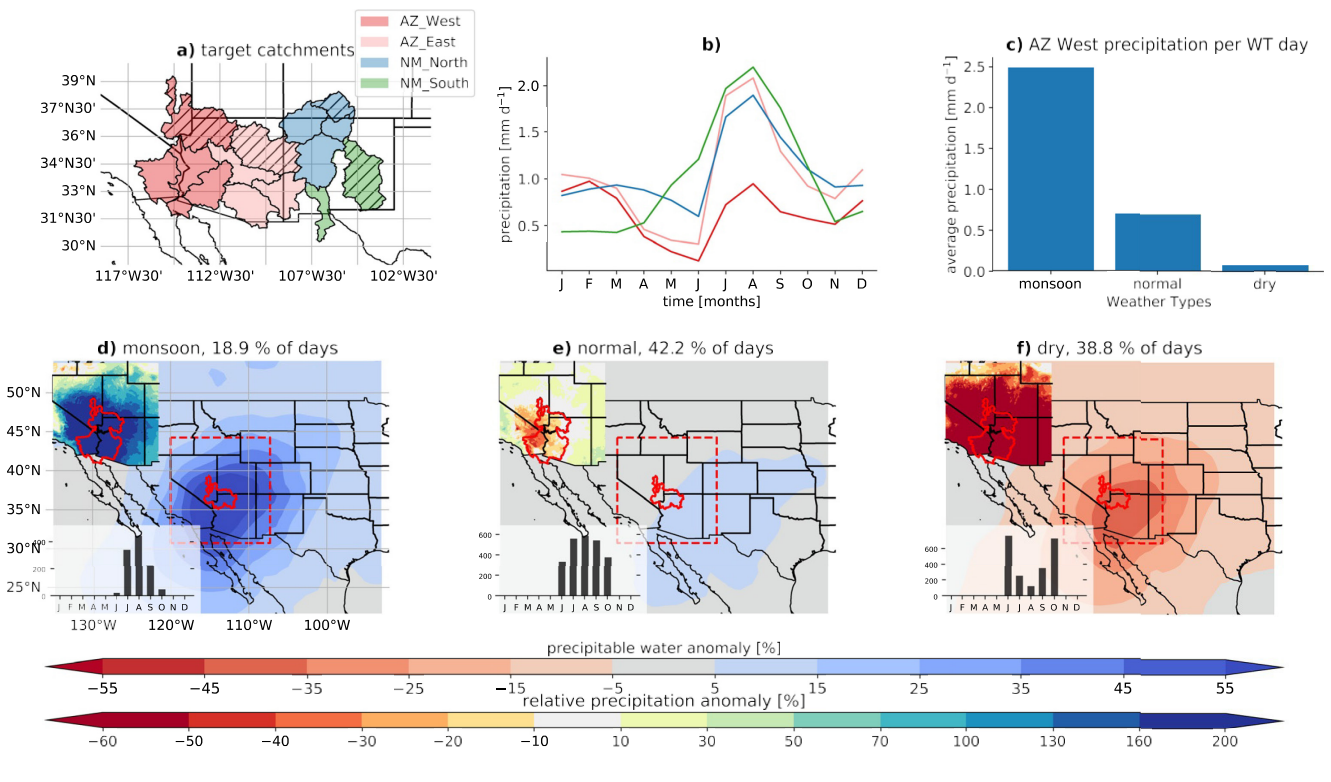


Figure 1. Three weather types—a wet (monsoon), normal, and dry weather type (WT)—characterize the major modes of synoptic-scale variability during the North American monsoon season. (a) Basin clusters that feature similar WTs include Arizona West (AZ West, dark red), Arizona East (AZ East; light red), New Mexico North (NM North, blue), and New Mexico South (NM South, green). Hatching shows the basin that was used to derive the WTs. (b) Monthly average precipitation in each region. (c) Average June to October precipitation during monsoon (d), normal (e), and dry (f) days in the AZ West region. Average WT precipitable water anomalies (colored contour) for each WT (d-f) in the AZ West region (red contour). The histogram in the lower left shows the monthly frequency of WT days. The inset in the top left shows the precipitation anomaly for each WT and the WT frequency is shown in the title of each panel.

2.3. Weather Typing Methodology

The WT algorithm was modified from the one presented in (Prein & Mearns, 2021). In short, it is a data-driven clustering algorithm that tests atmospheric predictor combinations to find optimal WTs based on objective skill scores associated with NAM precipitation. The details of the WTing algorithm are outlined below.

All days between June and October within the period 1982–2018 are considered in the clustering. We consider all 12 above-mentioned variables and up to combinations of three variables (220 possible combinations) as predictors for catchment precipitation. First, we calculate daily anomalies from the mean climate state of each predictor on a grid cell basis and apply Gaussian spatial smoothing (sigma = 0.5) to remove small-scale variability from the predictor variables. Next, we normalize the anomalies by their regional average mean and daily standard deviation. The normalized anomaly fields are then clustered using the results of a hierarchical (using Ward's linkage on a condensed distance matrix) cluster algorithm as initial seed for a k-means clustering (Romesburg, 2004). The combination of these two cluster algorithms showed high skill in a WT intercomparison study (Schiemann & Frei, 2010) and was successfully applied to capture precipitation characteristics over the US (Prein et al., 2016) and weather conditions in other regions (Comrie, 1996; Ekstrom et al., 2002).

For each catchment, we assess how these skill scores change if WTs from the remaining 13 basins are used as predictors of the selected catchment's NAM precipitation (Figure S1 in Supporting Information S1). In Arizona, using the WTs from the two northernmost catchments (Lower Colorado-Lake Mead subregion—HUC1501; Little Colorado subregion—HUC1502) results in higher skill in characterizing precipitation in southern (upwind during NAM conditions) catchments. Based on these results we cluster the catchments in Arizona in two regions—Arizona West (AZ West containing HUC1501, HUC1503, HUC1507, HUC1810) and Arizona East (AZ East containing HUC1502, HUC1504, HUC1506, HUC1508). Similarly, we cluster the catchments in New

PREIN ET AL. 3 of 11

Mexico into Northern catchments (NM North containing HUC1301, HUC140801, HUC130201, HUC130202) and southern catchments (NM South containing HUC130301 and HUC1306). The differences between Arizona and New Mexico WTs is not surprising since previous literature showed that spatial variability of monsoon precipitation differs east and west of the U.S. continental divide (Castro et al., 2012; Ciancarelli et al., 2014).

We derive clusters for each of the 14 target catchments (Figure 1a) and test the sensitivity of the cluster domain size by adding 2°, 5°, and 10° around a rectangle that includes the catchment of interest to test sensitivities to the clustering region (Beck et al., 2016).

We use two skill scores to assess the quality of derived WTs dependent on the predictor variables and WT domain size. The first is the absolute average of WT centroid (cluster mean state) precipitation anomalies (PR_{anom}), which should be maximized—the precipitation in the derived WTs should be as different as possible from the climatological precipitation. The second skill score is the ratio of the intra- versus inter-cluster standard deviation of precipitation (IvI), which should also be maximized. Although these two scores are correlated (Figure S2 in Supporting Information S1) combining them helps to improve the robustness of the derived WTs. This score favors WTs that have days with similar precipitation within WTs and whose precipitation is different between WTs. The combination of these two scores has been successfully used in previous WTing applications (Prein et al., 2016).

Based on these skill scores we select the top 10% of the tested predictor combinations and count how often each variable is included in a well-performing setting (Figure S3 in Supporting Information S1). Water vapor mixing ratio at 850 hPa (Q850) is by far the most frequently used predictor in well-performing settings in all catchments and results in close to optimal performance as a single predictor. Performance differences between different WT domain sizes are small but adding 5° around each catchment performed best in Arizona catchments and adding 2° was best in New Mexico. WTs are derived for each basin based on ERA-Interim data. The WT centroids are then use to associate each day in the seasonal forecasts to the most similar WT centroid according to their Euclidean distance.

2.4. Seasonal Prediction Systems

We use seasonal forecasts from the North American Multi-Model Ensemble (NMME; Kirtman et al., 2014) and the Integrative Forecasting System (IFS, Version 5) seasonal forecasts from ECMWF from the Copernicus Climate Change Service. We included all NMME models that provide daily Q850 for their hindcast (retrospective forecasts) runs, which are: NCAR CESM1, UM-RSMAS CCSM4, and ECMWF IFS. We also include NASA-GMAO GEOS-5 and CCCMA CanCM4 but use Q650 and Q675 respectively instead due to missing data at the 850 hPa level. This should have little impact on the predictive skill of those models since moisture patterns are well correlated between the 850 hPa and 650 hPa level (absolute differences do not matter due to the use of daily anomalies in the WTing). All models have a horizontal grid spacing of one degree. NMME models run a ten-member ensemble forecast while ECMWF runs 25 members. All models are initialized on the first of each month and forecast 365 days except for NASA-GMAO GEOS-5 and ECMWF IFS, which forecast 273 and 215 days respectively. The common hindcast period for the NMME models is 1982–2010 while ECMWF IFS provides hindcasts for 1993–2016.

To associate seasonal forecasts days with one of the derived WTs we use the same pre-processing as described above (i.e., for the predictor variables we derive daily anomalies, apply spatial smoothing, and normalize the anomalies). Next, we regrid the ERA-Interim based WT centroids to the one-degree model grid and calculate Euclidean distances to all WTs for each forecast day. A forecast day is assigned to a WT according to the lowest Euclidean Distance. We use linearly detrended time series for calculating anomaly correlation coefficients.

3. Results

Monsoon season (June–October) precipitation contributes between 60% (AZ West) to 80% (NM South) to the annual rainfall in the four study areas (Figure 1b). The precipitation in this period typically comes from moisture surges from the Gulf of Mexico and tropical Pacific (Favors & Abatzoglou, 2013; Higgins et al., 1997) intercepted by dry periods. We aim to capture this variability with our WTing analysis.

PREIN ET AL. 4 of 11

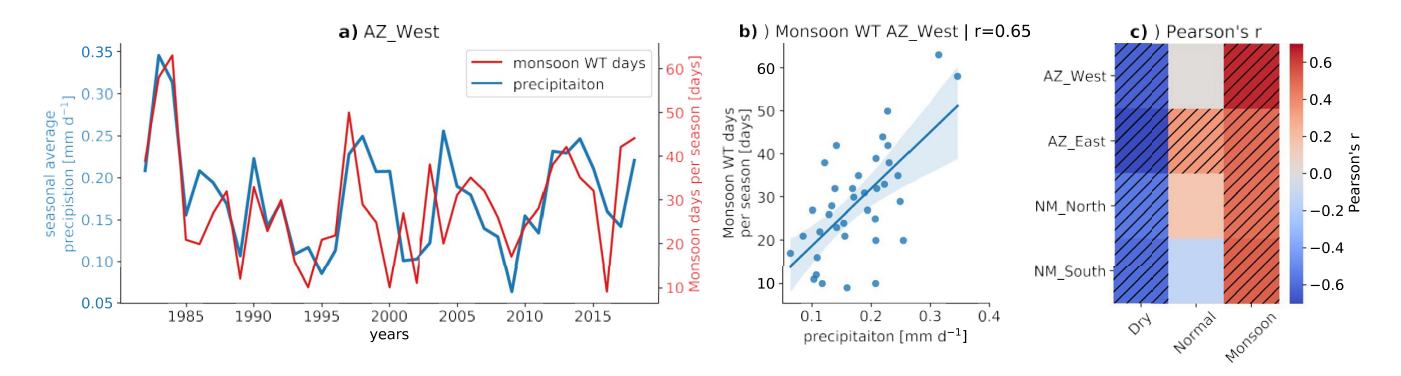


Figure 2. The frequency of North American monsoon season total monsoon weather type (WT) days is significantly correlated with seasonal catchment precipitation. (a) June to October daily average precipitation over the Arizona (AZ) West region (blue) and seasonal frequency of monsoon WT days (red) between 1982 and 2018. (b) Scatter plot and linear relationship estimate for the data shown in (a). The Pearson correlation coefficient is shown in the title. (c) Pearson correlation coefficient for all regions and WTs. Hatching indicated significant correlation coefficient (two-tailed *p*-value < 0.05).

3.1. Dominant Weather Types

Three weather patterns are sufficient to characterize the dominant effects of synoptic-scale variability on precipitation in the four target regions. The centroids of the three WTs in the AZ West region are shown in Figures 1d-1f. The first WT (monsoon) is associated with monsoonal moisture surges and characterized by tropical moisture advection from the Gulf of California and the eastern tropical Pacific further south into the target catchments resulting in a high water vapor mixing ratio at 850 hPa (Q850) and precipitable water anomalies. Monsoon WT days have a rapid onset in July, peak in August, and decay in September. This WT resembles the published definition of the NAM large-scale circulation and seasonal occurrence (Vera et al., 2006) and are often referred to as "moisture surges" (Pascale & Bordoni, 2016). Although only 19% of days within June to October are associated with this WT, they produce the majority of monsoon season precipitation (Figure 1c). Our definition of wet NAM days is more general than most published definition of synoptic patterns that cause wet surges. This is because we aim to used these patterns in a probabilistic predictive framework rather than understanding the drivers of wet surges in this region, which is already well studied (Higgins et al., 2004; Jiang & Lau, 2008; Schiffer & Nesbitt, 2012; Seastrand et al., 2015). Our wet WT definition includes the classical definition of wet surges but also allows capturing wet days with other synoptic-scale patterns (see Figure S13 in Supporting Information S1 and Movie S1 for an example). The second weather pattern (normal, Figure 1e) is associated with more zonal flow, a subtropical height that is weaker and centered on the coast of Texas, and climatologically average precipitable water anomalies. Days within this WT are 20%-40% dryer than average days and only contribute about one fifth of the precipitation of monsoonal flow days. The third WT (dry, Figures 1c and 1f) is associated with anomalously dry air advection, zonal flow, and extremely dry precipitation anomalies and resembles previously found dry patterns (Schiffer & Nesbitt, 2012). Dry WT days occur most frequently in June and October. Deriving WTs based on July-September conditions results in similar patterns (not shown), which indicates that these patterns are robust and inherent to the core monsoon season. An example of the occurrence of wet, normal, and dry WT days compared to daily average precipitation in the AZ West region for the dry 2009 and wet 2018 NAM season is shown in Figure S12 in Supporting Information S1.

The WTs for the other focus areas are shown in the supplement (Figures S4–S11 in Supporting Information S1). Each area features a monsoon, normal, and dry WT. The monsoonal WTs mainly differ in the size and location of the subtropical high-pressure system (Figure S15 in Supporting Information S1 shows 500 hPa geopotential height anomalies). The high-pressure system is shifted further to the east and south particularly in the NM North and South region, which facilitates the advection of Gulf of Mexico moisture rather than moisture from the Pacific as in the Arizona catchments.

The pronounced relationship between WTs and precipitation anomalies in the target regions results in a significant (Pearson's r = 0.65) correlation between the seasonal average frequency of monsoon WT days and observed monsoon season mean precipitation in the AZ west region (Figures 2a and 2b). Similarly high correlations are found in the other three regions (Figure 2c). Also, a high frequency of dry WT days is significantly negatively correlated with monsoon seasonal average precipitation.

PREIN ET AL. 5 of 11

19448007, 2022, 9, Downloaded from https://agupubs.onlinelibrary.wiley.com/doi/10.1029/2021GL095602, Wiley Online Library on [2804/2023]. See the Terms and Conditions (https://onlinelibrary.wiley.com/terms-and-conditions) on Wiley Online Library for rules of use; OA articles

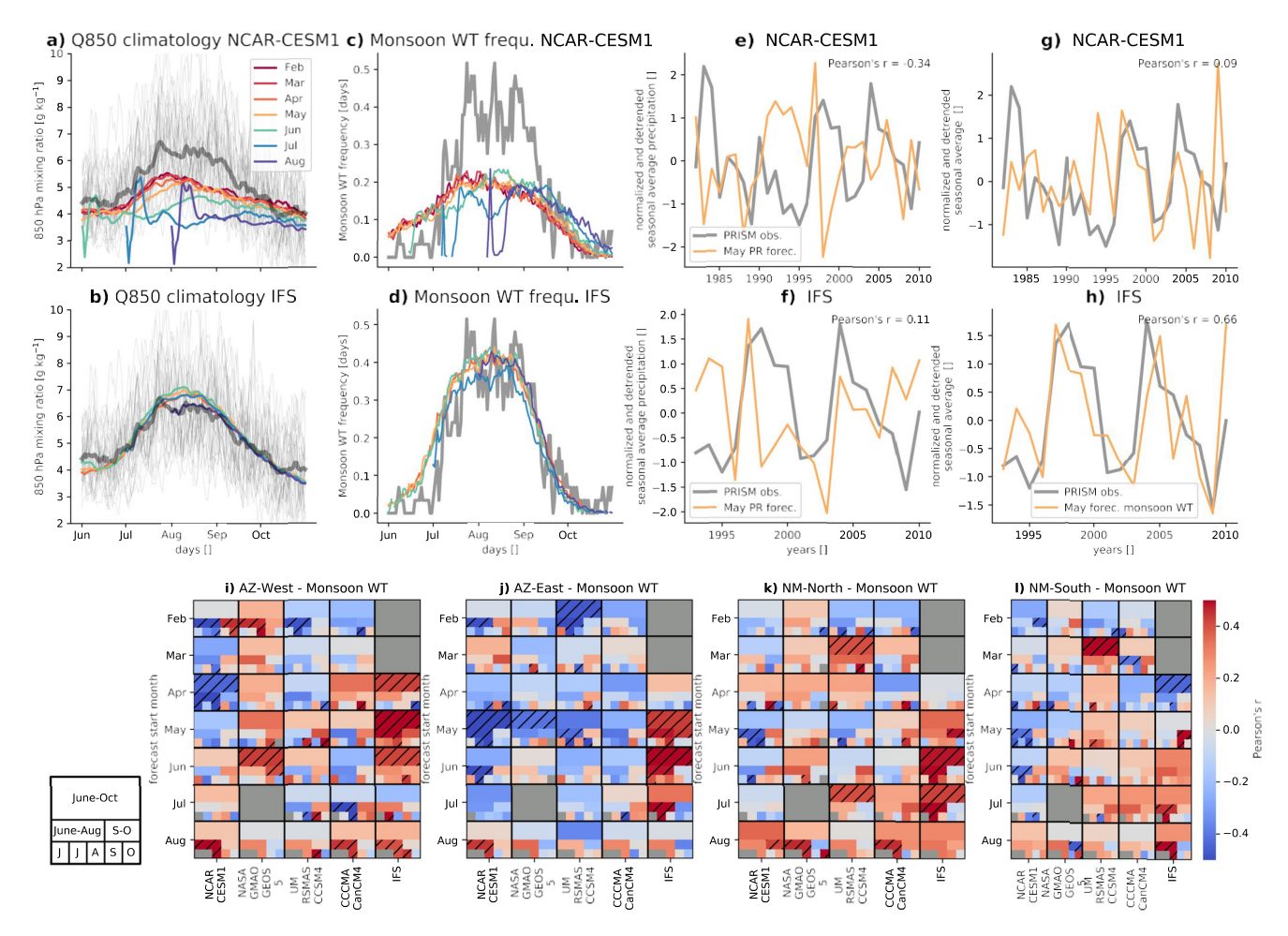


Figure 3. ECMWF's IFS model can skillfully forecast North American monsoon season precipitation starting in April when using monsoon weather type (WT) frequencies as a proxy for catchment average precipitation. ERA-Interim (gray), (a) NCAR-CESM1, and (b) ECMWF-IFS climatological average Q850 over the AZ West region. Thin gray lines show individual years from ERA-Interim and colors show different forecast initialization months. (c and d) Similar to (a and b) but for climatological average monsoon day frequencies. (e and f) Annual average detrended and normalized regional averaged observed (gray) and May forecast precipitation (orange). (g and h) Similar to (e and f) but for May forecast average detrended and normalized monsoon day frequency (orang) versus observed precipitation. (i–l) Heatmaps showing the Pearson correlation coefficient between the detrended and normalized observed basin average precipitation and forecasted monsoon WT frequency. Panels (i–l) show results from the AZ West, AZ East, NM North, and NM South watershed (from left to right). Each panel shows results from each modeling system (columns) and forecast start months (rows). Each month and model segment (see explanation on the bottom left) shows correlation coefficients for June–October (top two rows), June–August and September–October (second row from below), and each month (bottom row). Hatching indicates significant correlation coefficients (p < 0.1).

3.2. Seasonal Forecasts of Monsoon Precipitation in Hindcasts

There are large differences between the performance of the analyzed models in simulating the position and seasonal evolution of the monsoonal high pressure system that partly depend on the lead time of the forecast (Figure S15 in Supporting Information S1). The ECMWF-IFS system has the best climatological representation of the monsoonal high, while the other models feature a too far northward extension and partly erroneous seasonal progression.

Also, the ability to simulate the seasonal evolution of Q850 over the AZ West WT domain strongly depends on the forecasting system and the forecast lead time (Figures 3a and 3b). National Center for Atmospheric Research's Community Earth System Model v1 (NCAR-CESM1) forecasts feature a dry bias in Q850 during the peak monsoon season. This is not necessarily a problem as long as this bias is systematic since we perform the WTing with Q850 anomalies. A more severe issue is the considerable initiation shock—visible in the June, July, and August forecasts—which typically has strong negative impacts on the forecast quality (Mulholland et al., 2015). Similar to the positioning of the monsoonal high, the ECMWF-IFS v5 model forecasts show a much better

PREIN ET AL. 6 of 11

climatological evolution of the Q850 seasonal cycle and do not feature an initialization shock. The other forecasting systems (not shown) feature initialization shocks that are typically not as severe as the ones in the NCAR-CESM1 system.

The quality of simulating climatological Q850 conditions is reflected in the model's ability to capture the frequency and seasonality of monsoonal flow WT days (Figure 3c and 3d and Figure S16 in Supporting Information S1). NCAR-CESM1 has too many monsoon WT days in June and too few during the peak monsoon season. The impacts of the initialization shock are also visible in the forecasted monsoon WT frequencies. IFS has a much better simulation of the amount and seasonality of monsoon WT days (Figure 3d) and generally outperforms any of the other forecasting systems (Figure S16 in Supporting Information S1).

Using the modeled precipitation for forecasting observed NAM season precipitation results in no significant skill—measured by the anomaly correlation coefficient (Figures 3e and 3f)—confirming results from previous studies (Slater et al., 2019). This is also true for using NAM season monsoon WT frequencies from the NCAR-CESM1 forecast (Figure 3g; and the other NMME models). However, using the May forecast from the IFS model allows us to skillfully predict monsoon season precipitation in the AZ West region (Figure 3h; Pearson's r = 0.66). Even the April forecast is skillful (Figure 3i). Predicting the precipitation in individual months is more challenging except for the July and August forecast, which are skillful in predicting precipitation during the first forecasting month. Generally, June to August precipitation is more predictable than September and October rainfall.

IFS has similar high skill in forecasting precipitation in the AZ East region (Figure 3j; except for the April forecast) compared to AZ West. Predictability is generally lower in New Mexico and skillfully forecasting NAM season precipitation in the NM North region becomes feasible in June (Figure 3k) while no significant predictability is found in the NM South region (Figure 3l).

3.3. Sources for Predictability

Here we investigate the potential sources of predictability that allow skillful sub-seasonal precipitation forecasts by the IFS model.

Compositing the top 25% of years (top 9 years out of 37) with the highest frequency of monsoonal flow WT days in June and July in the AZ West region show significant 500 hPa geopotential height anomalies that resemble a Rossby wave train with alternating high and low anomalies (Figure 4a). Using the top 10% of years results in similar patterns (not shown). We focus on June on July conditions since they have the highest predictability (see Figure 3). A similar pattern has been identified previously as driver of continental-scale precipitation variability in the U.S. (Castro et al., 2012; Ciancarelli et al., 2014). This pattern is associated with La Nina like tropical Pacific sea surface temperatures (Figure 4b), which is in line with some previous studies (Ciancarelli et al., 2014; Higgins & Shi, 2001) but in opposition to others (Grantz et al., 2007). The anomaly patterns change gradually when moving from the AZ-West to the NM-South region with the high anomaly over the CONUS moving eastward and weakening and the low anomalies in the Gulf of Alaska and near the Gulf of California becoming stronger (Figure S17 in Supporting Information S1).

None of the forecasting systems is able to capture these anomaly patterns perfectly although we should expect some differences due to the different simulation periods. The June forecasts from the IFS model resemble the observed pattern best (Figure 4I) while the model's April forecasts miss the low anomaly in the Gulf of Alaska but still feature a correctly but too weak high anomaly over the central U.S. (Figure 4k). Nevertheless, IFS's April forecast better captures the observed pattern than most of the models forecast in June. for example, the GEOS-5 model has too strong and negative connections to the tropical Pacific (Figure 4f) while CanCM4 has too strong positive connections (Figure 4j). Most models struggle with correctly simulating the positive height anomaly in the western U.S. and many models show fundamentally different patterns in their April forecasts compared to their June forecasts.

PREIN ET AL. 7 of 11

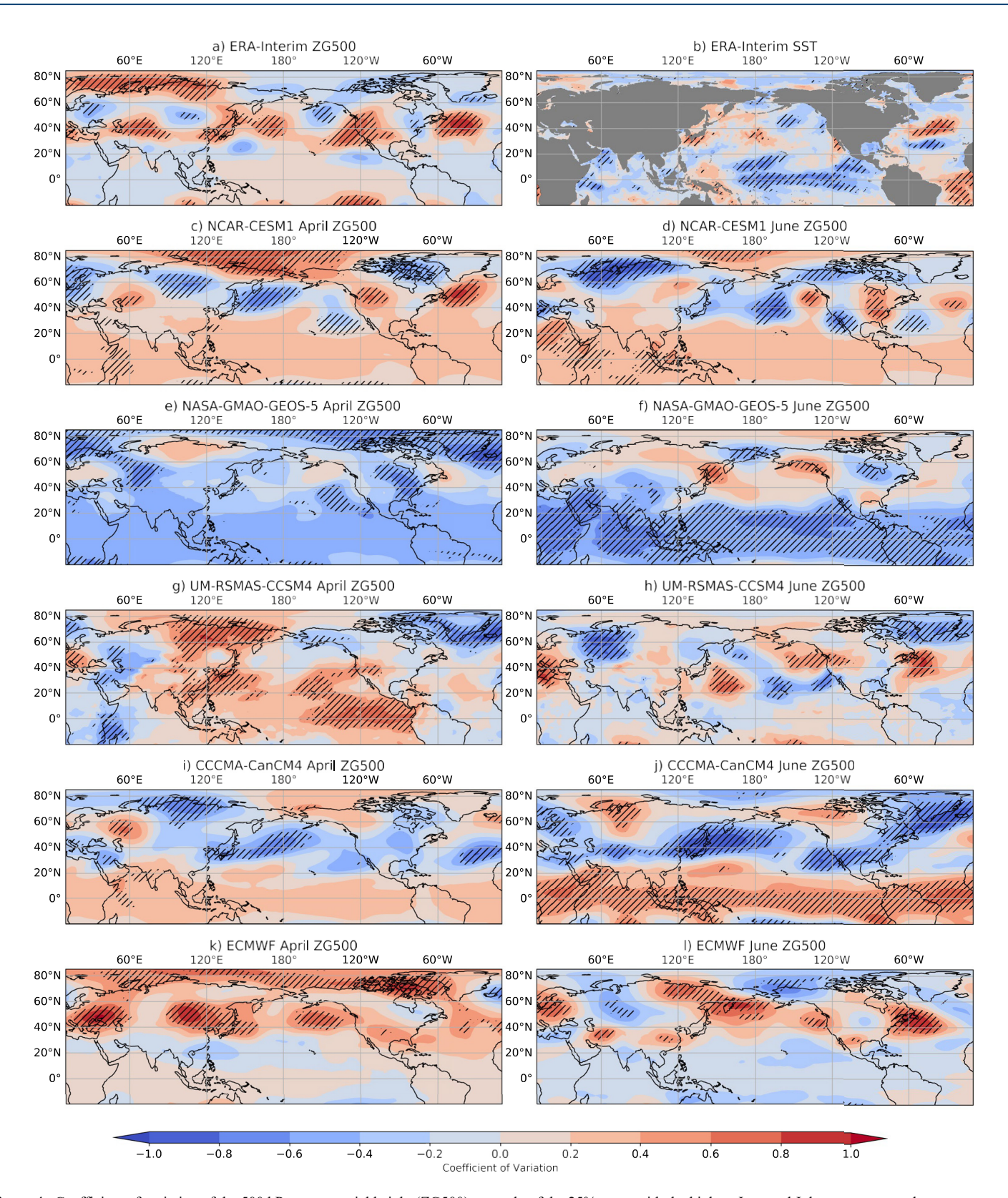


Figure 4. Coefficient of variation of the 500 hPa geopotential height (ZG500) anomaly of the 25% years with the highest June and July monsoon weather type frequencies compared to the climatological average. Shown is data from ERA-Interim (a; 1982–2018), the four included North American multi-model ensemble models (c–j; 1982–2010); and the ECMWF forecast (k–l; 1993–2016). Coefficients of variation are shown for April (left) and June (right) forecasts for each modeling system. Additionally, coefficient of variation of sea surface temperatures are shown based on ERA-Interim data (b). Hatched areas show significant anomalies based on the Mann-Whitney U test ($p \le 0.1$).

PREIN ET AL. 8 of 11

19448007, 2022, 9, Downloaded from

4. Discussion and Conclusion

We assess the ability of seasonal forecasting systems to predict the North American Monsoon (NAM, June to October) precipitation in Arizona and New Mexico catchments that are important for water management. Due to significant biases in simulating precipitation in state-of-the-art seasonal forecasting systems (Crochemore et al., 2016), we developed a forecasting framework that uses hydrologically important synoptic-scale weather types (WTs) for catchment-scale precipitation predictions. We found that three WTs—a dry, normal, and wet (monsoonal flow) WT—are sufficient to characterize the interseasonal and interannual variability of precipitation in the U.S. NAM region.

We show that the observed seasonal average frequency of monsoonal flow WTs significantly correlates with catchment-scale seasonal average precipitation in all regions. Most importantly, we show that ECMWF's IFS forecasting system can skillfully predict NAM season rainfall at catchment scales with several months lead-time (i.e., the April forecast is skillful over the AZ West catchments) except for the NM South catchments while using the model's precipitation as a predictor does not provide predictive skill. The other evaluated forecasting systems do not have predictive skills partly due to large initialization shocks (Mulholland et al., 2015), and an erroneous simulation of the low-level moisture transport into the study regions. Additionally, ECMWF-IFS has a superior simulation of the location and seasonal evolution of the monsoonal high pressure ridge and outperforms the other models in simulating teleconnection patterns (Castro et al., 2012; Ciancarelli et al., 2014) that control the position of the monsoon high and the amount of regional precipitation. The superior performance of the ECMWF-IFS system is not dependent on the use of ERA5 reanalysis data, since using MERRA2 data (Gelaro et al., 2017) results in similar seasonal and inter-annual WT properties (not shown).

These results push the boundaries of seasonal predictability of regional precipitation (Slater et al., 2019) and offer novel opportunities for improved water resource management on S2S time scales in the U.S. Southwest. The presented WTing framework is flexible and could offer enhanced predictive skill also for sub-seasonal forecasts and in other drought-prone regions around the world. The presented results also show that many S2S systems have to advance their data assimilation systems and reduce biases in their climatological representation of regional phenomena such as monsoon circulations. Having multiple prediction systems with the quality of ECMWF-IFS would allow us to construct more skillful multi-model ensemble forecasts resulting in further improvements of predictive skill. Importantly, even skillful models such as ECMWF-IFS are not able to simulate the mesoscale processes that drive local precipitation. Future research should focus on the potential added value of using convection-permitting models (Prein et al., 2015) for S2S prediction, which could result in a step-improvement in our skill to simulate mesoscale weather phenomena and their extremes (Clark et al., 2016; Prein et al., 2021), snowpack dynamics (Rasmussen et al., 2011), land-atmosphere interactions (Barlage et al., 2021), and could result in improved S2S predictive skills by better simulating teleconnections due to the dynamic interaction of convective scales with larger-scale processes (Weber & Mass, 2019).

Data Availability Statement

ERA-Interim (Dee et al., 2011) data can be accessed from https://apps.ecmwf.int/datasets/data/interim-full-daily/levtype=sfc/. The PRISM (Daly et al., 1997) precipitation data can be accessed from https://prism.oregonstate.edu/. NMME seasonal hindcasts (Kirtman et al., 2014) can be downloaded from https://www.ncdc.noaa.gov/data-access/model-data/model-datasets/north-american-multi-model-ensemble and ECMWF-IFS hindcasts and forecasts can be accessed from https://climate.copernicus.eu/seasonal-forecasts. The code for the statistical analysis and visualization of data in this document is published in A. F. Prein (2021).

References

Adams, D. K., & Comrie, A. C. (1997). The North American monsoon. Bulletin of the American Meteorological Society, 78(10), 2197–2213. https://doi.org/10.1175/1520-0477(1997)078<2197:tnam>2.0.co;2

Barlage, M., Chen, F., Rasmussen, R., Zhang, Z., & Miguez-Macho, G. (2021). The importance of scale-dependent groundwater processes in land-atmosphere interactions over the Central United States. *Geophysical Research Letters*, 48(5), e2020GL092171. https://doi.org/10.1029/2020gl092171

Beck, C., Philipp, A., & Streicher, F. (2016). The effect of domain size on the relationship between circulation type classifications and *surface climate*. https://doi.org/10.1002/joc.3688

Acknowledgments

This work was sponsored by the U.S. Bureau of Reclamation Interagency Agreements R20PG00065 and R20PG00083. We would like to acknowledge high-performance computing support from Cheyenne (https://doi.org/10.5065/D6RX99HX) provided by NCAR's Computational and Information Systems Laboratory. NCAR is sponsored by the National Science Foundation under Cooperative Agreement 1852977.

PREIN ET AL. 9 of 11

- Bureau of Reclamation, U. D. o. t. I. (2018). Annual operating plan for Colorado river reservoirs 2019. Tech. Rep. Retrieved from https://www.usbr.gov/lc/region/g4000/aop/AOP19.pdf
- Bureau of Reclamation, U. D. o. t. I. (2021). Glen canyon dam adaptive management program. Accessed July 8, 2021.
- Carleton, A. M. (1986). Synoptic-dynamic character of "bursts" and "breaks" in the South-West US summer precipitation singularity. *Journal of Climatology*, 6(6), 605–623. https://doi.org/10.1002/joc.3370060604
- Carleton, A. M., Carpenter, D. A., & Weser, P. J. (1990). Mechanisms of interannual variability of the southwest United States summer rainfall maximum. *Journal of Climate*, 3(9), 999–1015. https://doi.org/10.1175/1520-0442(1990)003<0999:moivot≥2.0.co;2</p>
- Castro, C. L., Chang, H.-I., Dominguez, F., Carrillo, C., Schemm, J.-K., & Henry Juang, H.-M. (2012). Can a regional climate model improve the ability to forecast the North American monsoon? *Journal of Climate*, 25(23), 8212–8237. https://doi.org/10.1175/jcli-d-11-00441.1
- Castro, C. L., McKee, T. B., & Pielke Sr, R. A. (2001). The relationship of the North American monsoon to tropical and North Pacific Sea surface temperatures as revealed by observational analyses. *Journal of Climate*, 14(24), 4449–4473. https://doi.org/10.1175/1520-0442(2001)014<449:trotna>2.0.co;2
- Ciancarelli, B., Castro, C. L., Woodhouse, C., Dominguez, F., Chang, H.-I., Carrillo, C., & Griffin, D. (2014). Dominant patterns of US warm season precipitation variability in a fine resolution observational record, with focus on the southwest. *International Journal of Climatology*, 34(3), 687–707. https://doi.org/10.1002/joc.3716
- Clark, P., Roberts, N., Lean, H., Ballard, S. P., & Charlton-Perez, C. (2016). Convection-permitting models: A step-change in rainfall forecasting. Meteorological Applications, 23(2), 165–181. https://doi.org/10.1002/met.1538
- Comrie, A. C. (1996). An all-season synoptic climatology of air pollution in the US-Mexico border region. *The Professional Geographer*, 48(3), 237–251. https://doi.org/10.1111/j.0033-0124.1996.00237.x
- Crochemore, L., Ramos, M.-H., & Pappenberger, F. (2016). Bias correcting precipitation forecasts to improve the skill of seasonal streamflow forecasts. Hydrology and Earth System Sciences, 20(9), 3601–3618. https://doi.org/10.5194/hess-20-3601-2016
- Daly, C., Taylor, G., & Gibson, W. (1997). The PRISM approach to mapping precipitation and temperature. In *Proc., 10th AMS conf. on applied climatology* (pp. 20–23).
- Dee, D., Uppala, S., Simmons, A., Berrisford, P., Poli, P., Kobayashi, S., et al. (2011). The ERA-Interim reanalysis: Configuration and performance of the data assimilation system. *Quarterly Journal of the Royal Meteorological Society*, 137(656), 553–597. https://doi.org/10.1002/gi.828
- Ekstrom, M., Jonsson, P., & Barring, L. (2002). Synoptic pressure patterns associated with major wind erosion events in southern Sweden. Climate Research, 23, 51–66. https://doi.org/10.3354/cr023051
- Favors, J. E., & Abatzoglou, J. T. (2013). Regional surges of monsoonal moisture into the southwestern United States. Monthly Weather Review, 141(1), 182–191. https://doi.org/10.1175/mwr-d-12-00037.1
- Gelaro, R., McCarty, W., Suárez, M. J., Todling, R., Molod, A., Takacs, L., et al. (2017). The modern-era retrospective analysis for research and applications, version 2 (MERRA-2). *Journal of Climate*, 30(14), 5419–5454. https://doi.org/10.1175/jcli-d-16-0758.1
- Grantz, K., Rajagopalan, B., Clark, M., & Zagona, E. (2007). Seasonal shifts in the North American monsoon. *Journal of Climate*, 20(9), 1923–1935. https://doi.org/10.1175/jcli4091.1
- Griffin, D., Woodhouse, C. A., Meko, D. M., Stahle, D. W., Faulstich, H. L., Carrillo, C., et al. (2013). North American monsoon precipitation reconstructed from tree-ring latewood. *Geophysical Research Letters*, 40(5), 954–958. https://doi.org/10.1002/grl.50184
- Gutzler, D. S., & Preston, J. W. (1997). Evidence for a relationship between spring snow cover in North America and summer rainfall in New Mexico. Geophysical Research Letters, 24(17), 2207–2210. https://doi.org/10.1029/97gl02099
- Higgins, R., Mo, K., & Yao, Y. (1998). Interannual variability of the US summer precipitation regime with emphasis on the southwestern monsoon. *Journal of Climate*, 11(10), 2582–2606. https://doi.org/10.1175/1520-0442(1998)011<2582:ivotus>2.0.co;2
- Higgins, R., & Shi, W. (2000). Dominant factors responsible for interannual variability of the summer monsoon in the Southwestern United States. *Journal of Climate*, 13(4), 759–776. https://doi.org/10.1175/1520-0442(2000)013<0759:dfrfiv>2.0.co;2
- Higgins, R., & Shi, W. (2001). Intercomparison of the principal modes of interannual and intraseasonal variability of the North American monsoon system. *Journal of Climate*, 14(3), 403–417. https://doi.org/10.1175/1520-0442(2001)014<0403:iotpmo>2.0.co;2
- Higgins, R., Shi, W., & Hain, C. (2004). Relationships between Gulf of California moisture surges and precipitation in the southwestern United States. *Journal of Climate*. 17(15), 2983–2997. https://doi.org/10.1175/1520-0442(2004)017<2983:rbgocm>2.0.co;2
- Higgins, R., Yao, Y., & Wang, X. (1997). Influence of the North American monsoon system on the US summer precipitation regime. *Journal of Climate*, 10(10), 2600–2622. https://doi.org/10.1175/1520-0442(1997)010<2600:iotnam>2.0.co;2
- Higgins, R. W., Chen, Y., & Douglas, A. V. (1999). Interannual variability of the North American warm season precipitation regime. *Journal of Climate*, 12(3), 653–680. https://doi.org/10.1175/1520-0442(1999)012<0653:ivotna>2.0.co;2
- Ikeda, K., Rasmussen, R., Liu, C., Newman, A., Chen, F., Barlage, M., et al. (2021). Snowfall and snowpack in the Western US as captured by convection permitting climate simulations: Current climate and pseudo global warming future climate. Climate Dynamics, 57(7), 2191–2215. https://doi.org/10.1007/s00382-021-05805-w
- Jiang, X., & Lau, N.-C. (2008). Intraseasonal teleconnection between North American and Western North Pacific monsoons with 20-day time scale. Journal of Climate, 21(11), 2664–2679. https://doi.org/10.1175/2007jcli2024.1
- Kirtman, B. P., Min, D., Infanti, J. M., Kinter, J. L., Paolino, D. A., Zhang, Q., et al. (2014). The North American multimodel ensemble: Phase-1 seasonal-to-interannual prediction; phase-2 toward developing intraseasonal prediction. Bulletin of the American Meteorological Society, 95(4), 585–601. https://doi.org/10.1175/bams-d-12-00050.1
- Krishnamurti, T., Stefanova, L., Chakraborty, A., Tsv, V., Cocke, S., Bachiochi, D., & Mackey, B. (2002). Seasonal forecasts of precipitation anomalies for North American and Asian monsoons. *Journal of the Meteorological Society of Japan. Ser. II*, 80(6), 1415–1426. https://doi.org/10.2151/jmsj.80.1415
- Lehner, F., Deser, C., & Terray, L. (2017). Toward a new estimate of "Time of emergence" of anthropogenic warming: Insights from dynamical adjustment and a large initial-condition model ensemble. *Journal of Climate*, 30(19), 7739–7756. https://doi.org/10.1175/jcli-d-16-0792.1
- Li, S., & Robertson, A. W. (2015). Evaluation of submonthly precipitation forecast skill from global ensemble prediction systems. Monthly Weather Review, 143(7), 2871–2889. https://doi.org/10.1175/mwr-d-14-00277.1
- Liu, J., Yang, H., Gosling, S. N., Kummu, M., Flörke, M., Pfister, S., et al. (2017). Water scarcity assessments in the past, present, and future. Earth's Future, 5(6), 545–559. https://doi.org/10.1002/2016ef000518
- MacDonald, G. M. (2010). Water, climate change, and sustainability in the southwest. *Proceedings of the National Academy of Sciences*, 107(50), 21256–21262. https://doi.org/10.1073/pnas.0909651107
- Mekonnen, M. M., & Hoekstra, A. Y. (2016). Four billion people facing severe water scarcity. *Science Advances*, 2(2), e1500323. https://doi.org/10.1126/sciadv.1500323

PREIN ET AL. 10 of 11

- Milly, P. C., & Dunne, K. A. (2020). Colorado River flow dwindles as warming-driven loss of reflective snow energizes evaporation. *Science*, 367(6483), 1252–1255. https://doi.org/10.1126/science.aay9187
- Mote, P. W., Hamlet, A. F., Clark, M. P., & Lettenmaier, D. P. (2005). Declining mountain snowpack in Western North America. Bulletin of the American Meteorological Society, 86(1), 39–50. https://doi.org/10.1175/bams-86-1-39
- Mulholland, D. P., Laloyaux, P., Haines, K., & Balmaseda, M. A. (2015). Origin and impact of initialization shocks in coupled atmosphere–ocean forecasts. *Monthly Weather Review*, 143(11), 4631–4644. https://doi.org/10.1175/mwr-d-15-0076.1
- Pascale, S., & Bordoni, S. (2016). Tropical and extratropical controls of Gulf of California surges and summertime precipitation over the south-western United States. *Monthly Weather Review*, 144(7), 2695–2718. https://doi.org/10.1175/mwr-d-15-0429.1
- Prein, A., Rasmussen, R., Wang, D., & Giangrande, S. (2021). Sensitivity of organized convective storms to model grid spacing in current and future climates. *Philosophical Transactions of the Royal Society A*, 379(2195), 20190546. https://doi.org/10.1098/rsta.2019.0546
- Prein, A. F. (2021). NAM S2S predictability. Retrieved from https://github.com/AndreasPrein/NAM S2S predictability
- Prein, A. F., Holland, G. J., Rasmussen, R. M., Clark, M. P., & Tye, M. R. (2016). Running dry: The US Southwest's drift into a drier climate state. Geophysical Research Letters, 43(3), 1272–1279. https://doi.org/10.1002/2015gl066727
- Prein, A. F., Langhans, W., Fosser, G., Ferrone, A., Ban, N., Goergen, K., et al. (2015). A review on regional convection-permitting climate modeling: Demonstrations, prospects, and challenges. Reviews of Geophysics, 53(2), 323–361. https://doi.org/10.1002/2014rg000475
- Prein, A. F., & Mearns, L. O. (2021). US Extreme precipitation weather types increased in frequency during the 20th century. *Journal of Geophysical Research: Atmospheres*, 126(7), e2020JD034287. https://doi.org/10.1029/2020jd034287
- Raff, D., Brekke, L., Werner, K., Wood, A., & White, K. (2013). Short-term water management decisions: User needs for improved climate, weather, and hydrologic information. Tech. Rep. U.S. Army Corps of Engineers. Retrieved from https://www.usbr.gov/research/st/roadmaps/WaterSupply.pdf
- Rasmussen, R., Liu, C., Ikeda, K., Gochis, D., Yates, D., Chen, F., et al. (2011). High-resolution coupled climate runoff simulations of seasonal snowfall over Colorado: A process study of current and warmer climate. *Journal of Climate*, 24(12), 3015–3048. https://doi.org/10.1175/2010icli3985.1
- Romesburg, C. (2004). Cluster analysis for researchers. Lulu. com.
- Schiemann, R., & Frei, C. (2010). How to quantify the resolution of surface climate by circulation types: An example for alpine precipitation. Physics and Chemistry of the Earth, Parts A/B/C, 35(9), 403–410. https://doi.org/10.1016/j.pce.2009.09.005
- Schiffer, N. J., & Nesbitt, S. W. (2012). Flow, moisture, and thermodynamic variability associated with Gulf of California surges within the North American monsoon. *Journal of Climate*, 25(12), 4220–4241. https://doi.org/10.1175/jcli-d-11-00266.1
- Seastrand, S., Serra, Y., Castro, C., & Ritchie, E. (2015). The dominant synoptic-scale modes of North American monsoon precipitation. *International Journal of Climatology*, 35(8), 2019–2032. https://doi.org/10.1002/joc.4104
- Slater, L. J., Villarini, G., & Bradley, A. A. (2019). Evaluation of the skill of North-American Multi-Model Ensemble (NMME) global climate models in predicting average and extreme precipitation and temperature over the continental USA. Climate Dynamics, 53(12), 7381–7396. https://doi.org/10.1007/s00382-016-3286-1
- Vera, C., Higgins, W., Amador, J., Ambrizzi, T., Garreaud, R., Gochis, D., et al. (2006). Toward a unified view of the American monsoon systems. Journal of Climate, 19(20), 4977–5000. https://doi.org/10.1175/jcli3896.1
- Weber, N. J., & Mass, C. F. (2019). Subseasonal weather prediction in a global convection-permitting model. *Bulletin of the American Meteorological Society*, 100(6), 1079–1089. https://doi.org/10.1175/bams-d-18-0210.1
- Yu, B., & Wallace, J. M. (2000). The principal mode of interannual variability of the North American monsoon system. *Journal of Climate*, 13(15), 2794–2800. https://doi.org/10.1175/1520-0442(2000)013<2794:tpmoiv>2.0.co;2
- Zhu, C., Lettenmaier, D. P., & Cavazos, T. (2005). Role of antecedent land surface conditions on North American monsoon rainfall variability. Journal of Climate, 18(16), 3104–3121. https://doi.org/10.1175/jcli3387.1

PREIN ET AL.